Validation of Early GOES-16 ABI On-orbit Geometrical Calibration Accuracy using SNO Method

Fangfang Yu*[a], Xi Shao[a], Xiangqian Wu[b], Vladimir Kondratovich[a] and Zhengping Li[c]
[a]ERT, Inc.@NOAA/NESDIS/STAR, College Park, MD, USA 20735; [b]NOAA/NESDIS/STAR, College Park, MD, USA 20735; [c]ASRC Federal, 7517 Mission Dr., Seabrook, MD 20706 USA

ABSTRACT

The Advanced Baseline Imager (ABI) onboard the GOES-16 satellite, which was launched on 19 November 2016, is the first next-generation geostationary weather instrument in the west hemisphere. It has 16 spectral solar reflective and emissive bands located in three focal plane modules (FPM): one visible and near infrared (VNIR) FPM, one midwave infrared (MWIR), and one longwave infrared (LWIR) FPM. All the ABI bands are geometeorically calibrated with new techniques of Kalman filtering and Global Positioning System (GPS) to determine the accurate spacecraft attitude and orbit configuration to meet the challenging image navigation and registration (INR) requirements of ABI data. This study is to validate the ABI navigation and band-to-band registration (BBR) accuracies using the spectrally matched pixels of the Suomi National Polar-orbiting Partnership (SNPP) Visible Infrared Imaging Radiometer Suite (VIIRS) M-band data and the ABI images from the Simultaneous Nadir Observation (SNO) images. The preliminary results showed that during the ABI post-launch product test (PLPT) period, the ABI BBR errors at the y-direction (along the VIIRS track direction) is smaller than at the x-direction (along the VIIRS scan direction). Variations in the ABI BBR calibration residuals and navigation difference to VIIRS can be observed. Note that ABI is not operational yet and the data is experimental and still under testing. Effort is still ongoing to improve the ABI data quality.

Keywords: GOES-16, Advanced Baseline Imager (ABI), geostationary, geometrical calibration accuracy, PLPT, SNO, SNPP/VIIRS.

1. INTRODUCTION

The first NOAA next-generation geostationary (GEO) weather satellite, GOES-R was successfully launched on 19 November 2016 and became GOES-16 on 30 November 2016 when it reached the geostationary orbit. The satellite is currently parking at 89.5°W at about 35,000km above the Equator undergoing a series of instrument performance and product tests. The main payload instrument on-board is Advanced Baseline Imager (ABI), which has 16 multispectral bands covering the spectrum between 0.47μm and 13.3 μm to provide continuous data stream for weather forecasting, disaster monitoring, and environmental and climatic change studies[1]. ABI Level-1B (L1B) data is produced in the Fixed-Grid which are a set of static pixel locations relative to an ideal geostationary satellite viewpoint. The angular separation between L1B imagery data pixels are 14, 28 and 56 μrad, which are corresponding to 0.5, 1.0, and 2.0 km at nadir, respectively[2]. Similar to Japan Meteorological Agency (JMA) Himawari-8 Advanced Himawari Imager (AHI) which was successfully launched on 7 October 2015 and became operational on 7 July 1015, the 16 spectral bands are located three focal plan models (FPM): 6 (band 1-6) at the visible and near-infrared (VNIR) FPM,5(Band 6-11) at the middle-wave infrared (MWIR) FPM, and 5 (Band 12-16) at the long-wave infrared (LWIR) FPM.

Compared to the precedent GOES Imagers, GOES-R series have a dramatic increase in Earth observation capabilities with 3 times spectral bands, 4 times the spatial resolution, 5 times the observation rate and "operate-through" requirement with more stringent image navigation and registration (INR) requirements. Brand new INR algorithms including using Kalman filtering and Global Positioning System (GPS) techniques for accurate on-orbit determination of attitude and orbit configuration are applied to ABI to meet the challenging mission objectives. To validate the ABI

*Fangfang.Yu@@noaa.gov; phone 1 301 683-2555

Earth Observing Systems XXII, edited by James J. Butler, Xiaoxiong (Jack) Xiong, Xingfa Gu, Proc. of SPIE Vol. 10402, 104020U · © 2017 SPIE · CCC code: 0277-786X/17/$18 · doi: 10.1117/12.2275196

INR performance, a large number of Landsat chips are used to assess and monitor the navigation, band-to-band registration (BBR), frame-to-frame registration (FFR), swath-to-swath registration (SSR), and within frame registration (WIFR) for the ABI L1B image products at different temporal scales[3]. In this study, we describe another method using collocated and near coincident SNPP Visible Infrared Imaging Radiometer Suite (VIIRS) M-bands images to independently validate the ABI navigation and registration accuracies at the sub-satellite area. The simultaneous nadir observations (SNO) of GOES-16 ABI and SNPP VIIRS provides the opportunity to inter-compare both the radiometric and geometric calibration differences between the two instruments.

2. DATA AND METHODOLOGY

The SNO spatial inter-comparison method was first introduced and described for the AHI and VIIRS I band in 2016[4]. Due to the low earth orbit (LEO) configuration, SNPP passes over the sub-satellite point (SSP) of the GEO satellites twice every 16 days, one in daytime and one in night. Once it overpassed the GEO SSP, both GEO and LEO instruments can view the nadir area within very similar viewing and illumination geometries and resulted in simultaneous nadir observations at the sub-satellite region. The coincident and collocated paired radiance in the SNO images have been widely used for the sensor-to-sensor radiometric inter-calibration for polar satellites[5]. The heterogeneous cloud and other surface structures in the SNO images also provide an opportunity to assess the navigation difference between two GEO and LEO bands and the BBR errors of GEO or LEO instruments. Assuming that the VIIRS M-band BBR error is smaller than that of ABI, we can use the VIIRS M-band as the reference to assess the ABI BBR error. When the time interval between the two satellites is very small and its impacts of the surface structure is negligible, the geo-location offset difference can then be used to assess the navigation difference between the two satellites. As the observation time difference increases (<7.5 minutes in this study), some surface structure difference caused by cloud and atmosphere movements may be observed in the ABI and VIIRS images. Yet all the VIIRS bands scan the same Earth surface. Same with the ABI images. The double difference technique, that is the difference in the geo-location offset in between the spectrally matched ABI and VIIRS bands (Table 1), can provide the BBR error for ABI bands, assuming that the VIIRS BBR error is negligible.

$$BBR_{i,j} = \left| Offset_{i,Mx} - Offset_{j,My} \right| \qquad (1)$$

where BBRi,j is the BBR error between ABI band *i* and band *j*; $Offset_{i,Mx}$ is the geo-location offset between ABI band *i* and VIIRS *Mx*. $Offset_{j,My}$ is the geo-location offset between ABI band *j* and VIIRS *My*. The BBR error between VIIRS *Mx* and *My* is considered as zero.

In the paper of Yu et al.[4], the 3 VIIRS I-band images were used as the reference to evaluate the AHI BBR accuracy. The mean radiance from 7x7 pixels centered at the collocated VIIRS pixels were calculated to represent the AHI radiance for the correlation assessment to determine the geo-location offset between AHI and VIIRS I-band images. To determine the geo-location offsets, the VIIRS images are shifted at the interval of I-band spatial resolution (375m) at cross and along-track directions. The result in general agrees with the JMA's operational INR validations. Yet this method may have two potential issues: 1) cannot determine the geo-location offset less than the I-band spatial resolution, and 2) Like ABI, each AHI L1B pixel in the fixed grid is also resampled from weighting samples within certain distance of the pixel location, not the mean radiance of the samples. To over these two potential shortcomings, in this study we further explore this method by shifting the VIIRS M-band images at its sub-pixel level using 2D Fast Fourier Transformation (FFT) function. The ABI resampler kernel and algorithm are used to simulate the ABI radiance from VIIRS data. In this study, each M-band image is shifted at 1/8 pixels, which is corresponding to about 94m of shift interval at both cross and along track directions.

The VIIRS instrument has 16 M bands which have a spatial resolution of 750m. Seven of the 16 M bands have similar spectral response functions (SRF) as the 2km spatial resolution ABI bands (Table 1). These seven ABI 2km resolution bands are located at the three FPMs: B05 and B06 at VNIR FPM, B07 and B11 at MWIR FPM, and B13, B14 and B15 at LMIR FPM. . In this study, only 6 imaging bands, B07, B11, B13, B14 and B15, are examined. The VIIRS geo-location calibration accuracy at nadir is about 0.1km[6]. We first subset the 1^ox1^o ABI image centered at the ABI SSP, and then subset the VIIRS nadir images which are slighter larger than the corresponding ABI geo-spatial location. The maximum time difference between ABI and VIIRS over the SSP is 7.5 minutes. For each ABI pixel at the subset image, identify the image coordinate location for the VIIRS pixel which is less than 750m

distance to the central location of the ABI pixel is identified and archived. Figure 1 shows an example of ABI B15 pixels over the VIIRS M16 SNO image on Feb. 28, 2017 at about 19:21UTC.

The VIIRS images are then shifted at along and cross track directions at sub-pixel interval using the 2D FFT function. After each along or cross track shift, the VIIRS pixels located within ±2 angular separation distances of the collocated pixel location are then considered as the samples used to resample the radiance for the corresponding collocated ABI pixel. The weight assigned to the sample is determined by its proximity distance to the collocated pixel. Correlation between the ABI and simulated ABI radiance is calculated after each sub-pixel shift. The shift with the maximum correlation values represents the geo-location offset between ABI and VIIRS. Currently the procedure of resampling after each shift is computer time consuming and effort is undergoing to fast the calculation speed.

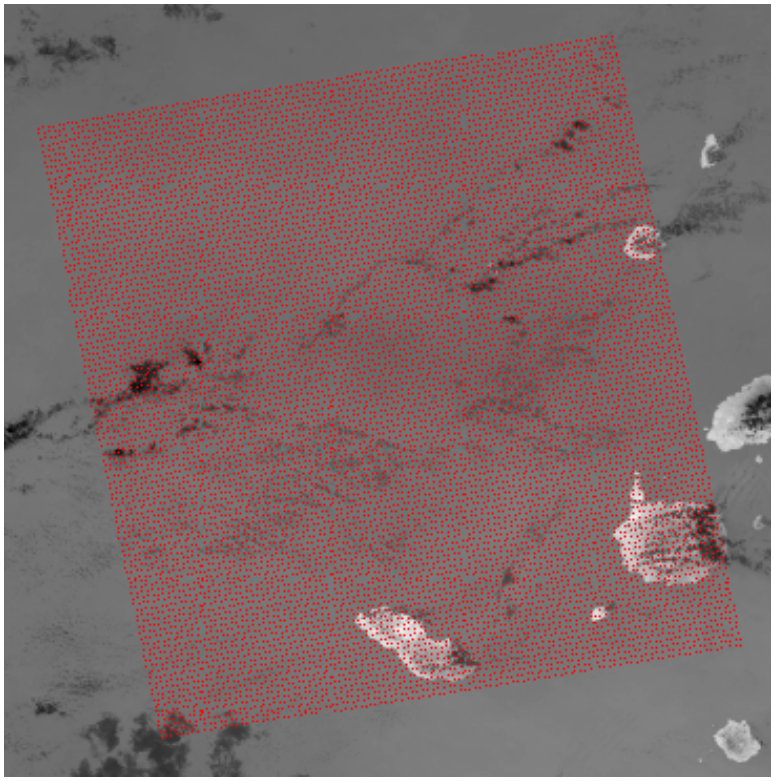

Figure 1. Geo-locations of collocated ABI B15 (12.3μm) pixels (in red) over the VIIRS M16 (12.0μm) for the SNO images obtained on Feb. 28, 2017 at about 19:21UTC).

Table 1. The spectrally paired ABI 2km and VIIRS M (750m) bands: names, central wavelength, and spatial resolutions

ABI		VIIRS	
Band Name	Central Wavelength	Band Name	Central Wavelength
B04	1.3μm	M09	1.3μm
B06	2.3μm	M11	2.3μm
B07	3.9μm	M12	3.7μm
B11	8.5μm	M14	8.6μm

B13	10.4μm	M15	10.8μm
B14	12.2μm	M15	10.8μm
B15	12.3μm	M16	12.0μm

3. RESULTS AND DISCUSSIONS

During the PLT/PLPT periods, ABI is undergoing a series tests with special scans. Only the full-disk (FD) ABI data are used to derive the SNO images for this study. As the results, a total of 11 SNO images are obtained from February through June (Table 2). For each spectrally paired images, correlation between the ABI pixels and the resampled VIIRS radiance is generated at each sub-pixel shift. In this study, the subpixel shift interval is set to 1/8 spatial resolution and the maximum shift distance is 4km at each direction. A typical correlation map between ABI B15 and VIIRS M16 is shown in Figure 2. The center coordinate represents the no shift of the VIIRS image. The distance between the maximum correlation location and the central coordinate is considered as the geo-location offset between the ABI and the VIIRS images. The x-direction represent for the VIIRS along-scan direction, y-direction for the VIIRS along-track direction.

Table 2. Time and time difference for the SNO events between February and June, 2017.

Day/month	02/10	02/12	02/28	03/14	03/16	04/01	05/01	06/02	06/04	06/18	06/20
UTC	07:19	19:21	19:26	07:21	19:21	19:23	07:15	07:15	19:15	07:15	19:15
Time difference (ABI-VIIRS) (in minute)	- 1.596	- 5.006	+ 2.773	+ 5.619	+ 2.806	+ 1.960	+ 0.085	- 2.727	- 2.727	+ 0.085	- 2.727

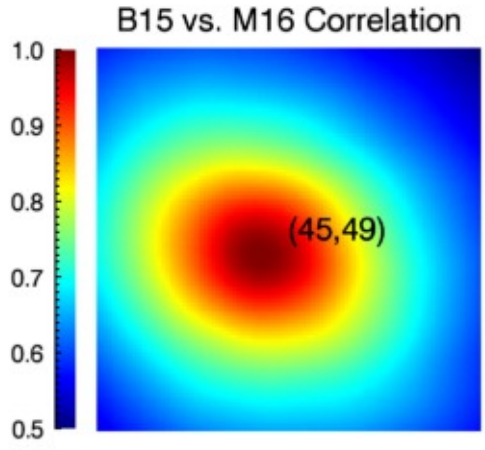

Figure 2. Correlation map between ABI B15 and simulated VIIRS M16 radiance for the SNO event on 02/28/2017. The image coordinate of the maximum correlation in this map is (45, 49), while the central coordinate is (53, 53), indicating that the geo-location offset between these two images is 0.75km in the along scan direction (x-direction), and 0.375km in the cross scan direction (y-direction)

3.1 ABI Band-to-Band Registration Error

Since the VIIRS BBR is very small (<0.1KM), its impacts on ABI BBR error can be considered negligible in this study. The ABI BBR error is calculated using the difference between geo-location offset. For each SNO event, the BBR errors between the 6 ABI imaging bands can be derived, except that there is no BBR for B06 for the night-time

SNO events. Figure 3 is an example of BBR errors at the x- and y- directions at the ABI SSP region on 20 June 2017 at 19:15UTC. The BBR errors are very small at less than 0.3km for all the bands studied at the y-direction, while they are relatively larger at the x direction. Some of the IR BBR errors at x-direction are larger than 1.0km.

6/20/2017 x - direction

B07					0.094
B11				0.938	1.031
B13			0.188	1.125	1.219
B14		0.188	0.375	1.313	1.406
B15	0.469	0.656	0.844	1.781	1.875
B15	B14	B13	B11	B07	B06

6/20/2017 y - direction

B07					0.094
B11				0.188	0.281
B13			0.094	0.094	0.188
B14		0.000	0.094	0.094	0.188
B15	0.094	0.094	0.000	0.188	0.281
B15	B14	B13	B11	B07	B06

Figure 3. ABI BBR errors on 06/20/2017.

Figure 4 and Figure 5 show two examples of time-series of BBR errors for B11 vs. B15 and B14 vs. B15, respectively. The BBR error at the y-direction is more variable than at the x-direction. As shown in Figure 3-5, the BBR residual could vary greatly at different band combination and time. Note that the y-direction is the along-track direction of VIIRS, which is not assigned with the NS direction of ABI image. The x-direction is the along scan direction of VIIRS. Adjustment of x-direction and y-direction of the BBR shift to the NS and EW directions in the ABI fixed-grid directions with the VIIRS orbit configuration information will be applied in the soon future.

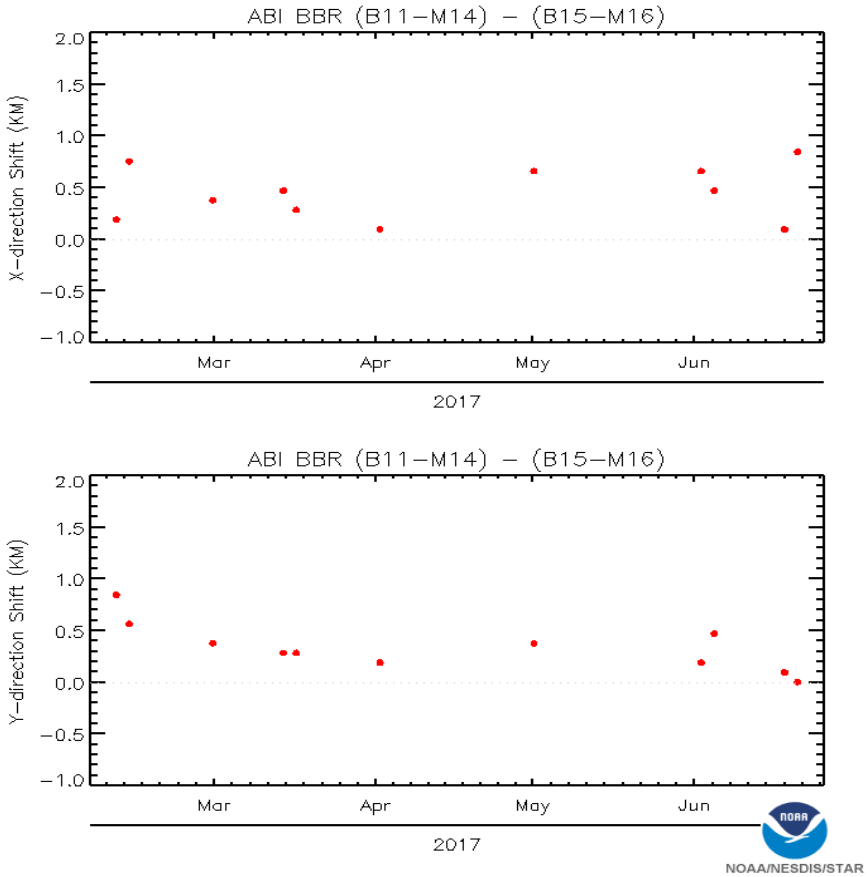

Figure 4. Time-series of ABI BBR error between ABI B11 and B15.

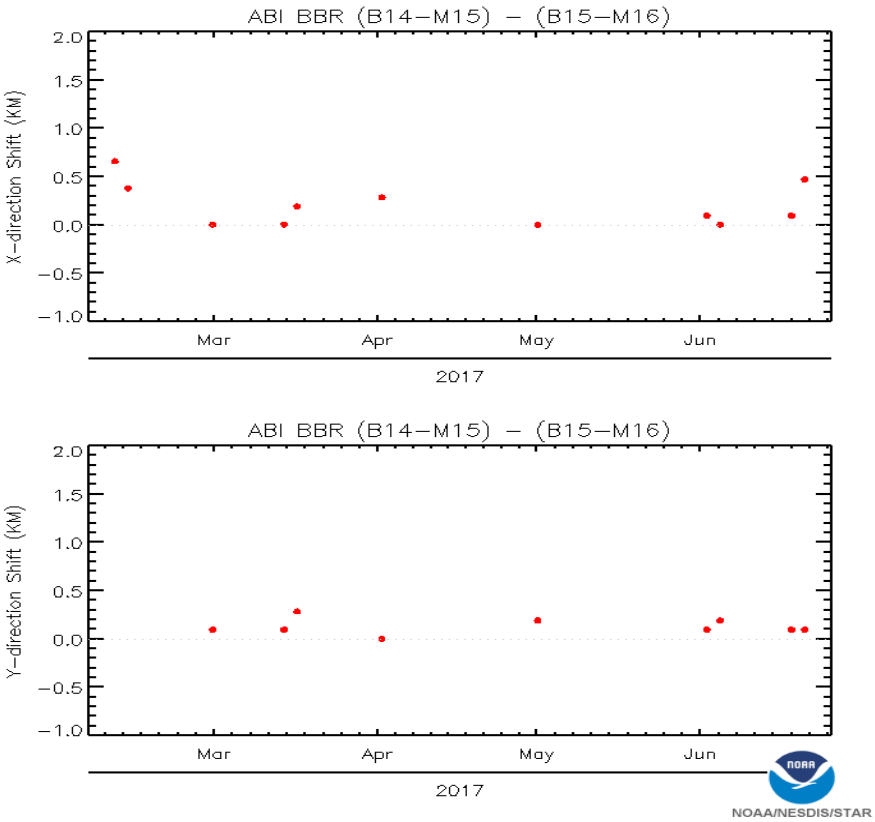

Figure 5. Same as Figure 4, but for ABI B14 vs. B15.

3.2 Navigation Difference between ABI and VIIRS

Table 2 shows that there are two night SNO events on 05/01/2017 and 06/18/2017 which have a mean time difference between ABI and VIIRS at less than 6 seconds. Assuming that there is no significant change of the earth surface structures within such short time difference, the geo-location offset between the ABI and VIIRS of these two SNO events provides two snap-shot navigation difference between these two instruments. As shown in Figure 6, the navigation difference at the y-direction is smaller than at the x-direction for these two cases.

4. SUMMARY

Brand new INR techniques are for the first time applied to the GEO weather instruments to meet the challenging requirements of the operational ABI L1B data. In this study, the ABI and VIIRS SNO images are used to independently assess the ABI navigation and band-to-band registration accuracy for the six ABI imaging bands located at three FPMs. This paper presents the method and results using the VIIRS M-bands images as the reference to assess the ABI INR. During the study period, the BBR error and navigation difference to VIIRS at the y-direction is generally smaller than at those at the x-direction. Variations of the INR can also be observed at the time-series plots. Same method is also applied to the SNO images for the VIIRS I-bands images. The INR validation results using VIIRS I-band as the reference agree well for those using VIIRS M-band data as the reference. The Landsat chips based INR validation also show relatively large BBR and navigation errors during the PLPT period. More work is still needed to validate the SNO results with the Landsat chips based INIR monitoring results. Note that GOES-16 is not operational yet. The ABI data is still experimental and under testing. Effort is still undergoing to improve the ABI data quality.

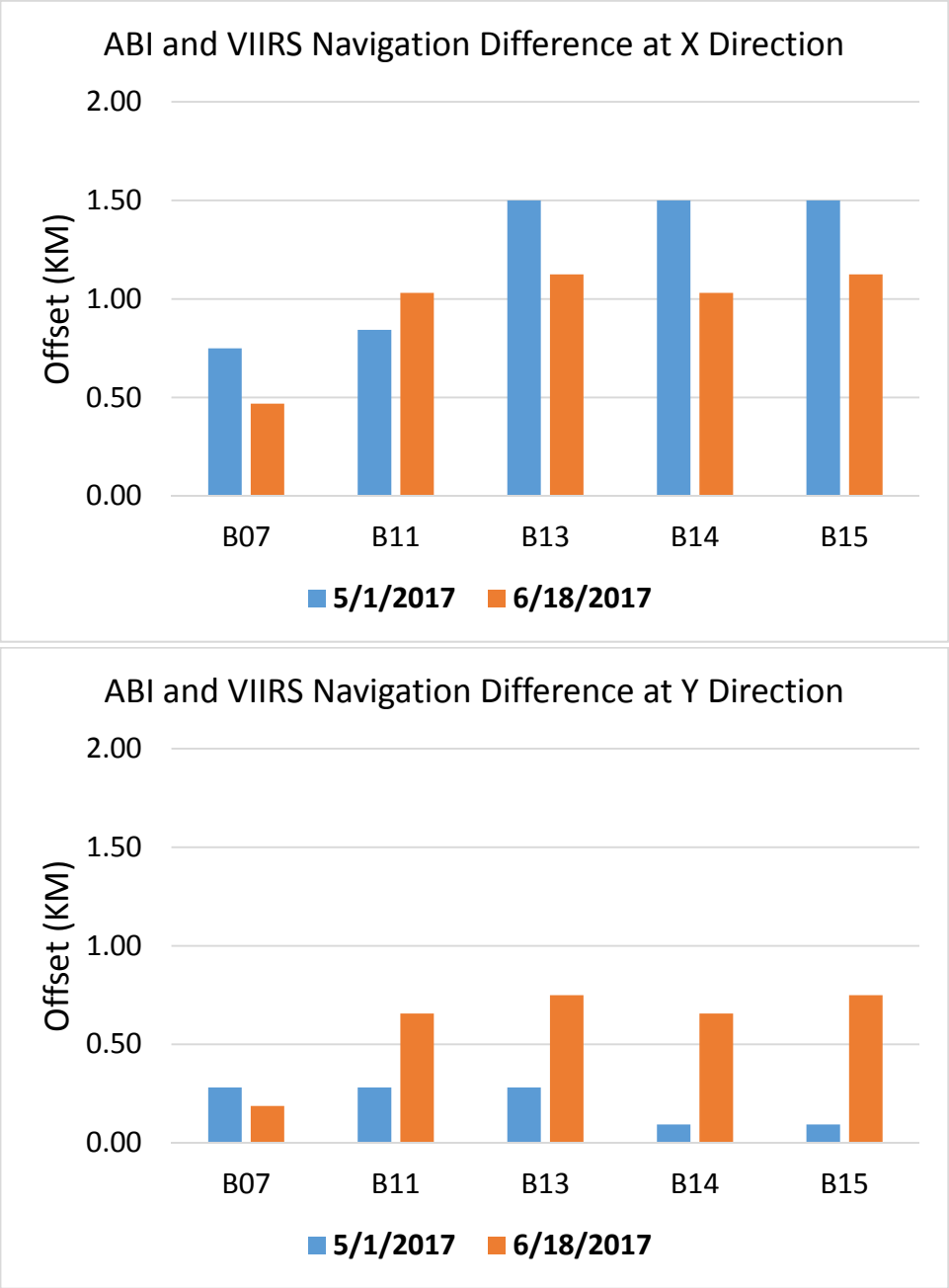

Figure 6. Navigation difference between ABI and VIIRS on 5/1/2017 and 6/18/2017. Upper: X-direction, lower: Y-direction.

ACKNOWLEDGEMENTS

This work is supported by NOAA GOES-R project. We would like to thank Dr. Bin Zhang for the discussion of SNPP VIIRS geometric calibration accuracy. This manuscript content is solely the opinions of the authors and do not constitute a statement of policy, decision, or position on behalf of NOAA or the U.S. government. GOES-16 satellite has not been declared operational and its data are preliminary and undergoing testing.

REFERENCES

[1] Schmit, T., Gunshor, M., Menzel, W.P., Gurka, J., Li, J. and Bachmeier, A.S., "Introducing the next-generation Advanced Baseline Imager on GOES-R," Bulletin of the American Meteorological Society, 1079-1096 (2005), doi:10.1175/BAMS-86-8-1079.

[2] Product Definition and Users' Guide (PUG), Vol 3: Level1B Products for GOES-R Series Core Ground Segment, Harris Corporation, Revision D, May (2015).

[3] Kondratovich, V., Zhu, L. and X. Wu, CWG weekly reports on the ABI INR performance, Feb – June (2017)

[4] Yu, F., Shao, X., Wu, X. and Krondratovich, V., "Evaluation of Himawari-8 AHI Geospatial calibration accuracy using SNP VIIRS SNO Data,", IGARSS, Beijing, July (2016).

[5] Cao, C., Xu, H., Sulliva, J., McMillin, L., Cirren, P., and Hou, Y. "Intersatellite radiance biases for the High-Resolution Infrared Radiation Sounder (HIRS) on board NOAA-15, -16, and -17 from simultaneous nadir observations," Journal of Atmospheric and Oceanic Technology, 22, 381-391, (2005).

[6] Wolfer, R.E., Lin, G., Nishihama, M., Tewari, K.P., Tilton, J.C. and Isaacman, A.R., "Suomi NPP VIIRS prelaunch and on-orbit geometric calibration and characterization," Journal of Geophysical Research, 118, 11,508-11,521, (2013).